

Numerical Simulation of Pulsed Gravel Packing Completion in Horizontal Wells

Zhenxiang Zhang¹, Jin Yang^{1,*}, Shengnan Chen², Qibin Ou¹, Yichi Zhang¹, Ximo Qu¹ and Yafei Guo³

¹ College of Safety and Ocean Engineering, China University of Petroleum, Beijing 102249, China; zzxcup1026@163.com (Z.Z.); cyjin1018@vip.sina.com (J.Y.); ouqibincup@163.com (Q.O.); czhangyc@163.com (Y.Z.); qxm19960129@163.com (X.Q.);

² Department of Chemical and Petroleum Engineering, University of Calgary, Calgary T2N1N4, Canada; snchen@ucalgary.ca (S.C.);

³ SINOPEC Yanshan Company, Beijing 102500, China; guoyf111.yssh@sinopec.com (Y.G.);

* Correspondence: cyjin1018@vip.sina.com

Abstract: Gravel packing completion method for horizontal wells has the advantages of maintaining high oil production for a long time, maintaining wellbore stability and preventing sand production, so it has become the preferred completion method for horizontal wells. At present, this technology still faces the problems of high sand bed height and poor gravel migration. In order to improve the efficiency of gravel packing in horizontal wells, pulsed gravel packing technology for horizontal wells is proposed for the first time. Based on the mechanism of hydraulic pulse, the Eulerian model, RNG K- ϵ model and CFD model are used to simulate the solid-liquid two-phase flow. By optimizing the parameters such as frequency and amplitude of pulse waveform, the optimal pulse waveform of pulsed gravel packing in horizontal wells is determined. The effects of parameters such as sand-carrying fluid displacement, sand-carrying fluid viscosity, sand-carrying ratio, gravel particle size and string eccentricity on pulsed gravel packing in horizontal wells are studied, and the distribution law of gravel migration velocity and volume fraction in horizontal wells is obtained. According to the results, it can be seen that with the increase of displacement and viscosity of carrier fluid, the volume fraction of fixed bed and moving bed decreases gradually, while that of suspension bed increases gradually. With the increase of sand-carrying ratio, gravel particle size and string eccentricity, the volume fraction of fixed bed and moving bed increases gradually, while that of suspended bed decreases gradually. Comparing the effects of conventional gravel packing and pulsed gravel packing in horizontal wells, it can be concluded that the efficiency of pulsed gravel packing in horizontal wells is higher. The volume fraction of fixed bed and moving bed decreased by 30% and 40% respectively, while the volume fraction of suspended bed increased by 20%. The migration velocity of moving bed and suspended bed increased by 40% and 25% respectively. And the migration ability of gravel improved obviously.

Keyword: horizontal well; pulsed gravel packing; completion; solid-liquid two-phase flow

0 Introduction

With the rapid development of the petroleum industry, the advantages and remarkable economic benefits of using horizontal wells to exploit oil and gas fields have been paid more attention by all countries in the world, especially the exploitation of offshore oil fields with horizontal wells, which has a broader application prospect. **Error! Reference source not found.** The gravel packing completion method for horizontal wells has the advantages of maintaining high production of oil wells, maintaining wellbore stability, and preventing sand production from the formation for a long time **Error! Reference source not found.** Especially for unconsolidated sandstone reservoirs with severe sand production, the gravel packing completion method for horizontal wells is a sand control completion technology with good effect, which has become the preferred horizontal well completion method in modern oil wells **Error! Reference source not found.** However, the sand bed plugging problem still exists in gravel packing operation of horizontal wells, which hinders the large-scale application of gravel packing technology in horizontal wells.

For the above problems, there are many scholars have conducted a lot of research on the gravel packing technology of horizontal wells. Forrest **Error! Reference source not found.** established a gravel packing simulation experiment device to carry out experiments on the gravel packing process in the annulus of highly deviated wells and horizontal wells. Maly et al **Error! Reference source not found.** developed a gravel packing tool that can be used for vertical wells and inclined wells through laboratory experiments. A two-layer flow model of solid-liquid two-phase horizontal pipe flow was proposed by Doron et al [7,8], who considered that the lower part of the horizontal pipeline is flowing sand bed and the upper part is suspension. However, the disadvantage of this model is that the sand bed is supposed to be movable, which makes it hard to predict the formation of stationary sand bed. In order to overcome the shortcomings of the two-layer flow model, Doron and Barnea **Error! Reference source not found.** proposed a three-layer flow model of solid-liquid two-phase flow, which divided the pipe flow into three layers: suspension, flowing sand bed, and stationary sand bed. This model could predict the formation of the stationary sand bed and the concentration distribution of solid particles in suspension.

Gruesbeck et al [10] proposed the concept of "equilibrium bank" for the first time based on the results of laboratory gravel packing experiments and established mathematical models for inclined and horizontal wells under the condition of complete packing. This model can calculate the equilibrium height of sand bed, but it's not suitable for the condition of premature plugging. Peden et al [11,12,13] used the semi-empirical formula to analyze the experimental data of gravel packing in horizontal wells and found that the main factors affecting the packing efficiency were the diameter of the wellbore annulus, the density of the sand-carrying fluid, and the diameter of punching pipe. Since the calculation accuracy of the empirical formula depended on experimental data and experimental conditions, the calculation results of this model were less stable. Wahlmeier and Andrews [14]

divided the wellbore into many tiny units along the axis based on the finite difference method and proposed a quasi three-dimensional mathematical model of gravel packing in horizontal wells. Chen [15] compared three critical velocities according to the research results of Penberthy [16,17], and obtained the height range of α wave during gravel packing process. Osisanya et al [18] studied the sensitivity factors of gravel packing in the horizontal well and proposed a method for selecting parameters such as the diameter of wash pipe, solid concentration, the viscosity of sand-carrying fluid, and the flow rate of sand-carrying fluid. Based on the finite volume method, Nguyen et al [19] described the flow process of solid-liquid two-phase flow in the axial and radial direction by using three-dimensional numerical simulation. Martins et al [20] proposed a mathematical model to calculate the α wave deposition height based on the two-layer flow model of solid-liquid two-phase flow. Based on the solid-liquid two-phase flow theory, Pu [21] established an intelligent calculation system for gravel packing in horizontal wells, which considering formation leakage. Ojo et al [22,23] established a three-dimensional mathematical model of gravel packing in horizontal wells under the influence of multiple factors and predicted the balanced height of sand bed during gravel packing process in horizontal wells. When Dong et al [24,25,26] conducted a numerical simulation study on the gravel packing process in horizontal wells, they took into account the influences of sand-carrying fluid filtration to the formation and fluid mass exchange between wellbore annulus and scrubber annulus on gravel packing. They not only set up the mass conservation equation and momentum conservation equation of the gravel and sand-carrying fluid of two independent flow systems of wellbore annulus and scour annulus, but also set up the flow coupling equation of each system. To sum up, the calculation model of sand bed balance height obtained by laboratory experiment and numerical simulation has certain limitations in the field construction process of gravel packing in horizontal wells, because it is easy to occur that the sand bed height is too high, leading to gravel plugging string and packing failure. There is an urgent need for a new horizontal gravel packing method to improve gravel migration and increase the success rate of field operations.

In this paper, the pulsed gravel packing method for horizontal wells is proposed for the first time. This method based on the mechanism of hydraulic pulse, the Eulerian model, RNG $k-\varepsilon$ model, and CFD model are used to simulate the solid-liquid two-phase flow. By optimizing the parameters such as frequency and amplitude of pulsed gravel packing in horizontal wells, the best pulse waveform is obtained. Furthermore, the influences of the displacement of sand-carrying fluid, the viscosity of sand-carrying fluid, sand-carrying ratio, the diameter of gravel and the eccentricity of the string on gravel packing in horizontals well are studied. Comparing with conventional gravel packing, it is found that the pulsed gravel packing method in horizontal wells reduces the volume fraction of fixed sand bed and moving sand bed and improves the transport speed of moving sand bed and suspended sand bed, which proves the superiority of pulsed gravel packing in horizontal wells.

1 Pulsed gravel packing numerical model

1.1 Solid-liquid two-phase flow governing equation

Based on the Eulerian model [27], pulsed gravel packing in the horizontal well is studied in this paper. The model assumes that both liquid and solid phases are continuous, the density of both liquid and solid phases is constant, and there is no mass transfer. The continuity equation can be expressed as [28,29]:

$$\text{Liquid phase} \quad \frac{\partial}{\partial t}(\varepsilon_l \rho_l) + \nabla \times (\varepsilon_l \rho_l \vec{v}_l) = 0 \quad (1)$$

$$\text{Solid-phase} \quad \frac{\partial}{\partial t}(\varepsilon_s \rho_s) + \nabla \times (\varepsilon_s \rho_s \vec{v}_s) = 0 \quad (2)$$

Where, ε_l 、 ε_s represent the density of the liquid and solid phase, $\varepsilon_l + \varepsilon_s = 1$, [constant]; ρ_l 、 ρ_s represent the velocity of liquid and solid phase, [kg/m³]; \vec{v}_s 、 \vec{v}_s represent the velocity of the liquid phase and solid phase, [m/s].

Assuming that there is no mass exchange between the solid phase and the liquid phase, the momentum governing equations can be obtained as follows **Error! Reference source not found.** **Error! Reference source not found.**:

$$\text{Liquid phase} \quad \frac{\partial}{\partial t}(\varepsilon_l \rho_l \vec{v}_l) + \nabla \times (\varepsilon_l \rho_l \vec{v}_l \vec{v}_l) = \varepsilon_l \nabla \tau_1 + \varepsilon_l \rho_l \vec{g} - \varepsilon_l \nabla p + \beta (\vec{v}_l - \vec{v}_s) \bar{\tau}_1 \quad (3)$$

$$\text{Solid phase} \quad \frac{\partial}{\partial t}(\varepsilon_s \rho_s \vec{v}_s) + \nabla \times (\varepsilon_s \rho_s \vec{v}_s \vec{v}_s) = -\varepsilon_s \nabla p + \varepsilon_s \nabla \bar{\tau}_s + \varepsilon_s \rho_s \vec{g} - \beta (\vec{v}_l - \vec{v}_s) \quad (4)$$

The liquid phase stress tensor τ_1 as follow:

$$\bar{\tau}_1 = \mu_l \left[\nabla \vec{v}_l + (\nabla \vec{v}_l)^T \right] - 2/3 \mu_l (\nabla \vec{v}_l) \vec{I} \quad (5)$$

The solid phase stress tensor τ_s as follow:

$$\bar{\tau}_s = (-p_s + \xi_s \nabla \vec{v}_s) \vec{I} + \mu_s \left\{ \left[\nabla \vec{v}_s + (\nabla \vec{v}_s)^T \right] - \frac{2}{3} (\nabla \vec{v}_s) \vec{I} \right\} \quad (6)$$

Where, g is the acceleration of gravity, [m/s²]; p_l is the liquid pressure, [MPa]; p_s is the solid phase pressure, [MPa]; β is the drag force coefficient between liquid and solid phase, [dimensionless]; μ_l is the shear viscosity of liquid phase, [Pa·s]; μ_s is the shear viscosity of solid phase, [Pa·s]; ξ_s is the dynamic viscosity of solid phase, [Pa·s]; and \vec{I} is the unit vector.

In this paper, when CFD software is used for numerical simulation of gravel packing in horizontal wells, the turbulence model is the RNG k - ε model [31,32]. The transport equations of the turbulent kinetic energy k and turbulence dissipation rate ε of the fluid in the turbulence model can be expressed as follows [33,34]:

$$\rho_m \frac{\partial k}{\partial t} + \rho_m \nabla \cdot (\vec{v}_m k) = \nabla \cdot \left(\left(\mu_m + \frac{\mu_{t,m}}{\sigma_{kRNG}} \right) \nabla k \right) + G_{k,m} - \rho_m \varepsilon \quad (7)$$

$$\rho_m \frac{\partial \varepsilon}{\partial t} + \rho_m \nabla \cdot (\vec{v}_m \varepsilon) = \nabla \cdot \left(\left(\mu_m + \frac{\mu_{t,m}}{\sigma_{\varepsilon RNG}} \right) \nabla \varepsilon \right) + C_{1\varepsilon RNG} G_{k,m} \frac{\varepsilon}{k} - \rho_m C_{2\varepsilon RNG} \frac{\varepsilon^2}{k} \quad (8)$$

$$\rho_m = \sum_{i=1}^N \alpha_i \rho_i \quad (9)$$

$$\mu_m = \sum_{i=1}^n \alpha_i \mu_i \quad (10)$$

$$\vec{v}_m = \frac{\sum_{i=1}^N \alpha_i \rho_i \vec{v}_i}{\sum_{i=1}^N \alpha_i \rho_i} \quad (11)$$

$$\mu_{t,m} = C_{\mu\text{RNG}} \rho_m k^2 / \varepsilon \quad (12)$$

$$G_{k,m} = \mu_{t,m} \left(\nabla \vec{v}_m + (\nabla \vec{v}_m)^T \right) : \nabla \vec{v}_m \quad (13)$$

$$C_{1e\text{RNG}} = 1.42 - f_\eta \quad (14)$$

$$f_\eta = \frac{\eta \left(1 - \frac{\eta}{4.38} \right)}{(1 + \beta_{\text{RNG}} \eta^3)} \quad (15)$$

$$\eta = \sqrt{\frac{G_{k,m}}{\rho_m C_{\mu\text{RNG}} \varepsilon}} \quad (16)$$

Where, k is turbulent kinetic energy, $[\text{m}^2/\text{s}^2]$; ε is the dissipation rate of turbulent kinetic energy, $[\text{m}^2/\text{s}^2]$; ρ_m is the mixed density of two phases, $[\text{kg}/\text{m}^3]$; ρ_i is the density of phase i , $[\text{kg}/\text{m}^3]$; v_m is the mixed velocity of two phases, $[\text{m}/\text{s}]$; v_i is the velocity of phase i , $[\text{m}/\text{s}]$; α_i is the volume fraction of phase i , [dimensionless]; μ_m is the mixed dynamic viscosity of two phases, $[\text{Pa} \cdot \text{s}]$; $\mu_{t,m}$ is the mixed turbulent viscosity of two phases, $[\text{Pa} \cdot \text{s}]$; $G_{k,m}$ is the increment of turbulent kinetic energy caused by the average velocity gradient; $C_{1e\text{RNG}}$ is the turbulent kinetic energy coefficient, [dimensionless]; and the constants in the equation as follows: $C_{\mu\text{RNG}}=0.085$, $C_{2e\text{RNG}}=1.68$, $\sigma_{k\text{RNG}}=0.7179$, $\sigma_{\varepsilon\text{RNG}}=0.7179$, $\beta_{\text{RNG}}=0.012$.

1.2 Physical models and Boundary conditions

During the pulsed gravel packing process in horizontal wells [35], the sand-carrying fluid is transported to the horizontal section of the wellbore through the pipe string. When the sand-carrying fluid enters the annulus of the casing and sand control string, the gravel is gradually transported and deposited in the annulus, while the fluid is returned to the sand control string through the screen. A physical model is established for the gravel packing process of horizontal wells, as shown in Figure 1.

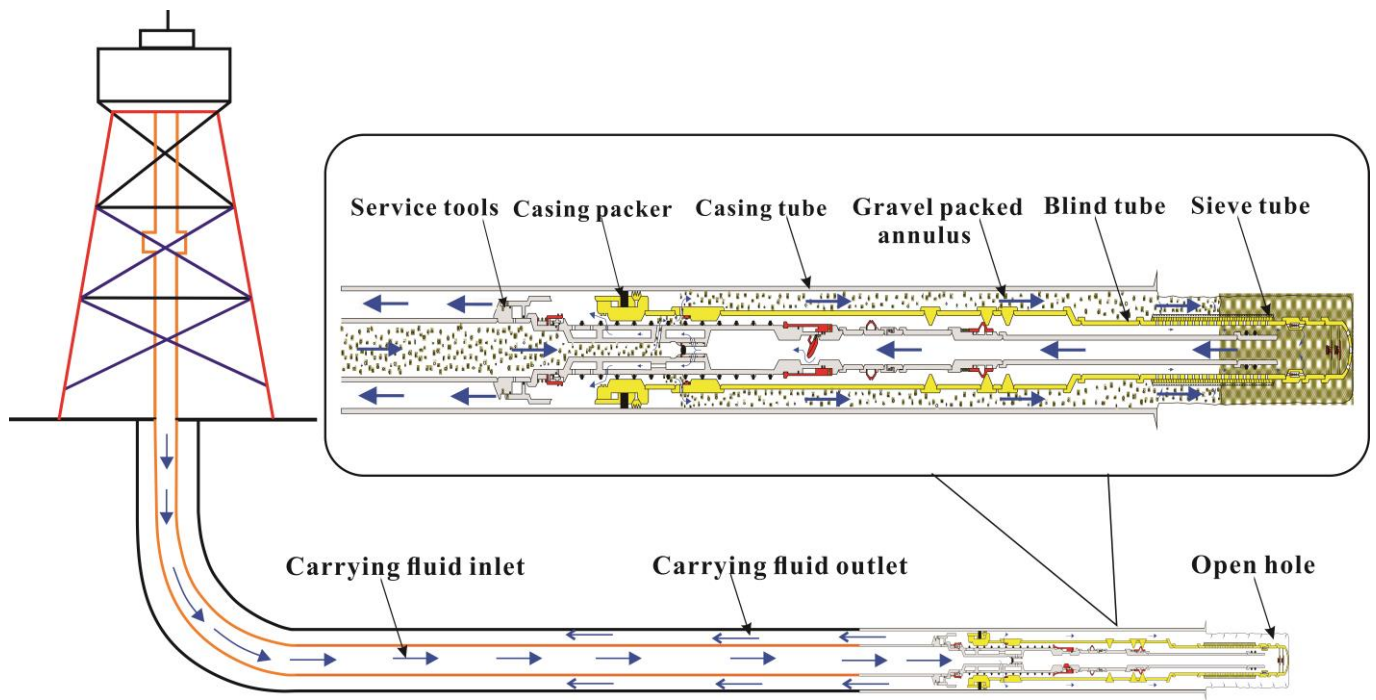


Figure 1. Schematic diagram of pulsed gravel packing in horizontal wells

By simplifying the physical model of the gravel packing process in the horizontal well, a finite element numerical model is established for the horizontal well section. The string diameter is 88.9 mm, the borehole diameter is 152.4 mm, and the model length is 20 m. The model is shown in Figure 2:

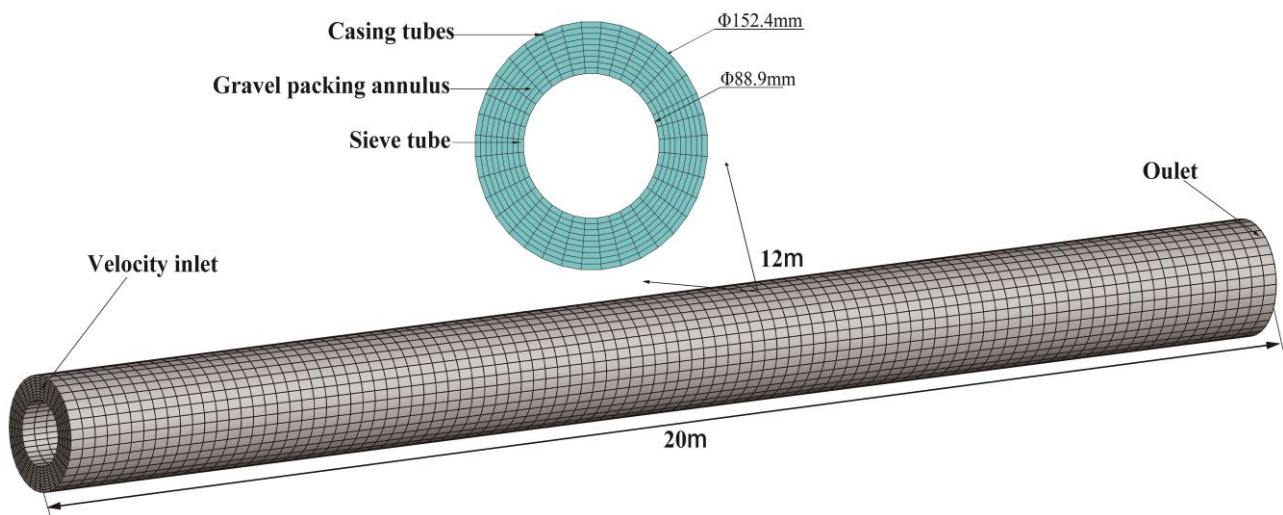


Figure 2. Numerical model of pulsed gravel packing in horizontal wells

In order to ensure the convergence and stability of the calculation results, the following assumptions are made for the boundary conditions of the numerical model:

(1) Velocity inlet boundary is adopted and UDF subroutine is introduced to realize the change of pulse waveform. At the same time, the influences of annulus temperature and bottom hole gas and water seepage on the flow of sand-carrying fluid are ignored, and the sand-carrying fluid is regarded as the incompressible fluid [36].

(2) The outlet boundary adopts the pressure boundary, and the boundary pressure value is consistent with

the environmental pressure.

(3) The string and wellbore are assumed to be smooth without slip boundary, and the gravel diameter and density are the same in any wellbore section.

2 Parameter analysis of pulsed gravel packing

2.1 Optimization of pulsed gravel packing parameters

In CFD software, the sinusoidal pulse waveform is defined by embedding the UDF program to change the inlet boundary velocity. According to the theory of sinusoidal pulse wave, the frequency range of the selected pulse waveform is 2.5~10 Hz, the amplitude range is 1.5~2.0 m/s. Numerical simulation is carried out by combination of frequency and amplitude, where the simulation time is 60 s, the average amplitude is 1 m/s, the initial sand-carrying ratio is 10%, the gravel diameter is 1 mm, the sand-carrying fluid viscosity is 1.0 mPa·s and the eccentricity of the string is 0. The evaluation criteria were fixed bed volume fraction and gravel migration velocity. Pulse waveforms with different amplitudes and frequencies are shown in Figure 3 and Figure 4 respectively.

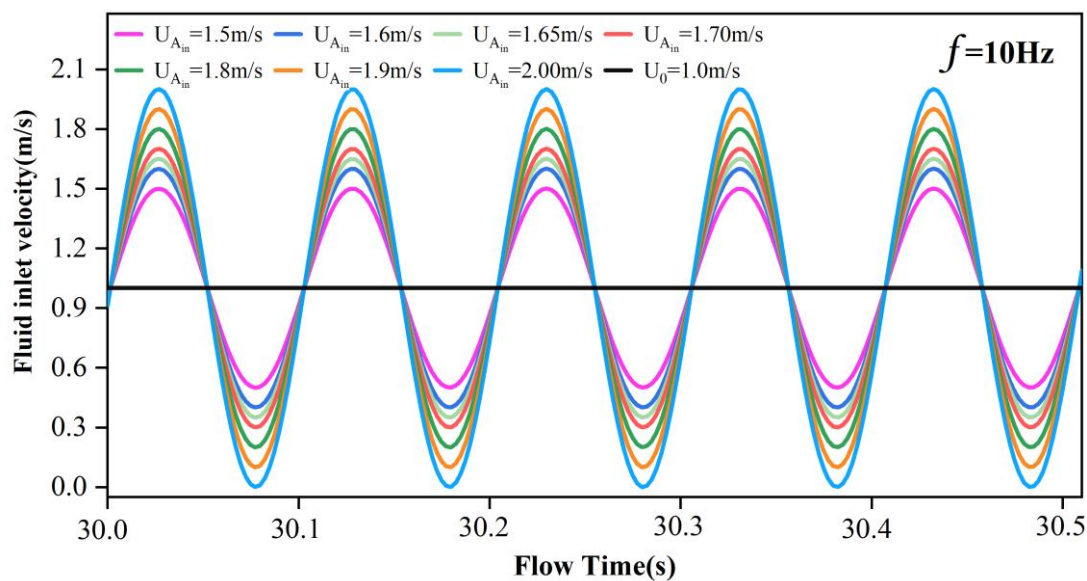


Figure 3. Graph of the pulse waveform with different amplitudes

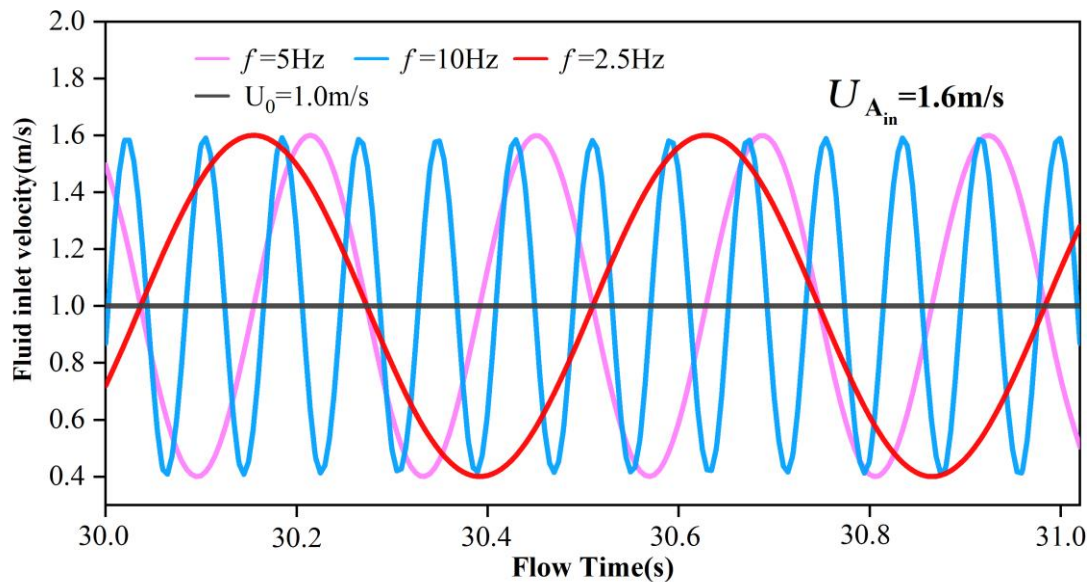


Figure 4. Graph of the pulse waveform with different frequencies

In the pulsed gravel packing process of horizontal wells, three layers of hydraulic flow may occur in annular flow field, which are fixed bed, moving bed and suspended bed respectively. As shown in **Error! Reference source not found..**

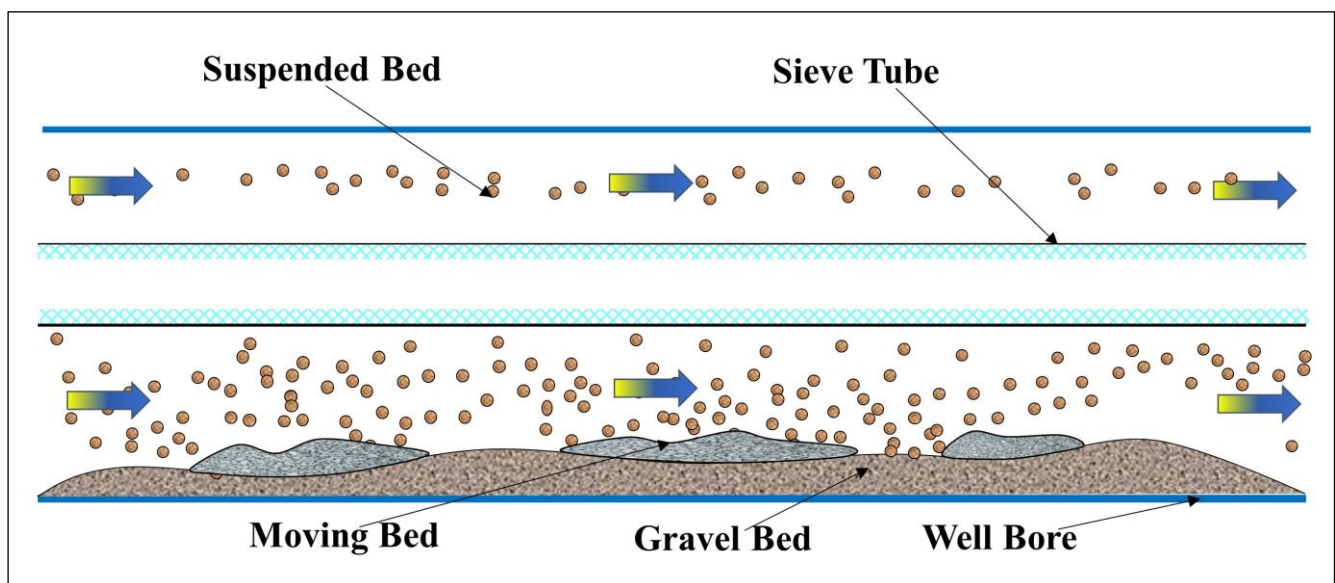


Figure 5. Schematic diagram of the three-layer hydraulic flow pattern during gravel migration process

2.2 Optimal Analysis of pulsed gravel packing waveform in horizontal wells

The numerical simulation of pulsed gravel packing horizontal wells is carried out with the frequency range of pulse waveform is 2.5Hz ~ 10Hz and the amplitude range is 1.5m /s~ 2.0m /s. The results are shown in Figure 6. When the frequency is 10 Hz, the volume fraction of the fixed bed increases from 2.78% to 11.85% with the increase of amplitude. When the frequency is 5 Hz, the volume fraction of fixed bed decreases first and then increases with the increase of amplitude, in which the minimum value is 1.14% and the maximum value is 8.77%. When the frequency is 2.5Hz, the volume fraction of the fixed bed also decreases first and then increases with

the increase of amplitude, in which the minimum volume fraction is 2.06% and the maximum volume fraction is 9.35%. Through comparative analysis, it is found that when the frequency is 5 Hz and the amplitude is 1.65 m/s, the volume fraction of the fixed bed is the smallest and its value is 1.144%. Under this combination of frequency and amplitude, the sand-carrying fluid not only has strong sand-carrying performance but also has the best effect of reducing the volume fraction of fixed bed. Therefore, the pulsed gravel packing method has less risk and higher filling efficiency during the packing process.

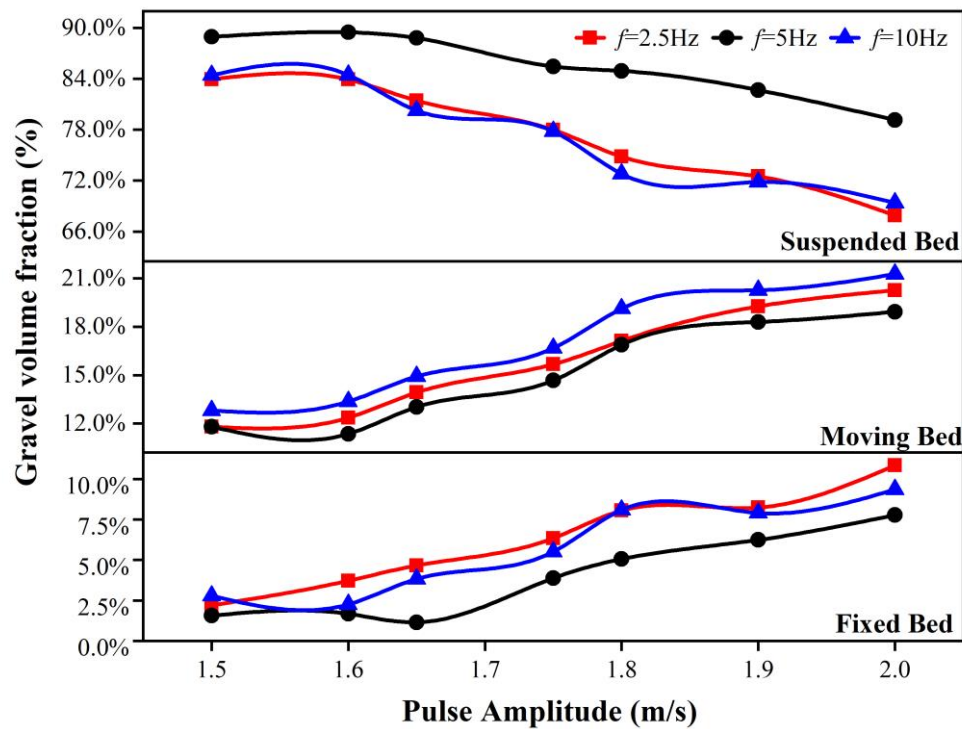


Figure 6. Graph of gravel volume fraction for pulsed gravel packing in horizontal wells

2.3 Comparative analysis of pulsed gravel packing and conventional gravel packing in horizontal wells

When the transport law of pulsed gravel packing and conventional gravel packing in horizontal wells is compared, the optimized pulse waveform parameters are added to the inlet boundary, and other influencing factors are consistent with the conventional gravel packing. Gravel migration velocity and gravel volume fraction were used as evaluation indexes. In order to explain the gravel migration for horizontal wells in detail, sections are established at 3 m, 5 m, 7 m, 10 m, 15 m, and 17 m from the inlet. At the same time, extracting the volume fraction and migration velocity of pulsed gravel packing and conventional gravel packing in horizontal wells at different locations at the time of 30 s, results as shown in Figure 7, Figure 8, and Figure 9. Under the same conditions, the volume fraction of fixed bed and moving bed with pulsed gravel packing in horizontal wells is smaller than that of conventional gravel packing, while the volume fraction of suspended bed is larger than that of conventional gravel packing. The gravel transport velocity of pulsed gravel packing in horizontal wells is faster. At the position of section 15 m, the volume fractions of fixed, mobile, and suspended beds with conventional gravel packing were 9.24%, 22.2%, and 68.56%, respectively. The volume fractions of the fixed bed, moving bed,

and suspended bed with pulsed gravel packing were 5.35%, 16.1%, 78.55%, respectively. It can be seen that the fixed bed volume fraction and moving bed volume fraction of pulsed gravel packing in horizontal wells decreased by 42.1% and 27.5% respectively, and the suspended bed volume fraction increased by 14.5%.

Research shows that pulsed gravel packing in horizontal wells is more efficient than conventional gravel packing, and the sand bed height decreases more significantly. Among them, the fixed bed volume fraction decreased by 30% on average, the mobile bed volume fraction decreased by 35% on average, the suspended bed volume fraction increased by 12% on average, and the gravel migration velocity increased by 40% on average. Pulsed gravel packing in horizontal wells increases the migration distance of gravel and greatly improves the success rate of gravel packing.

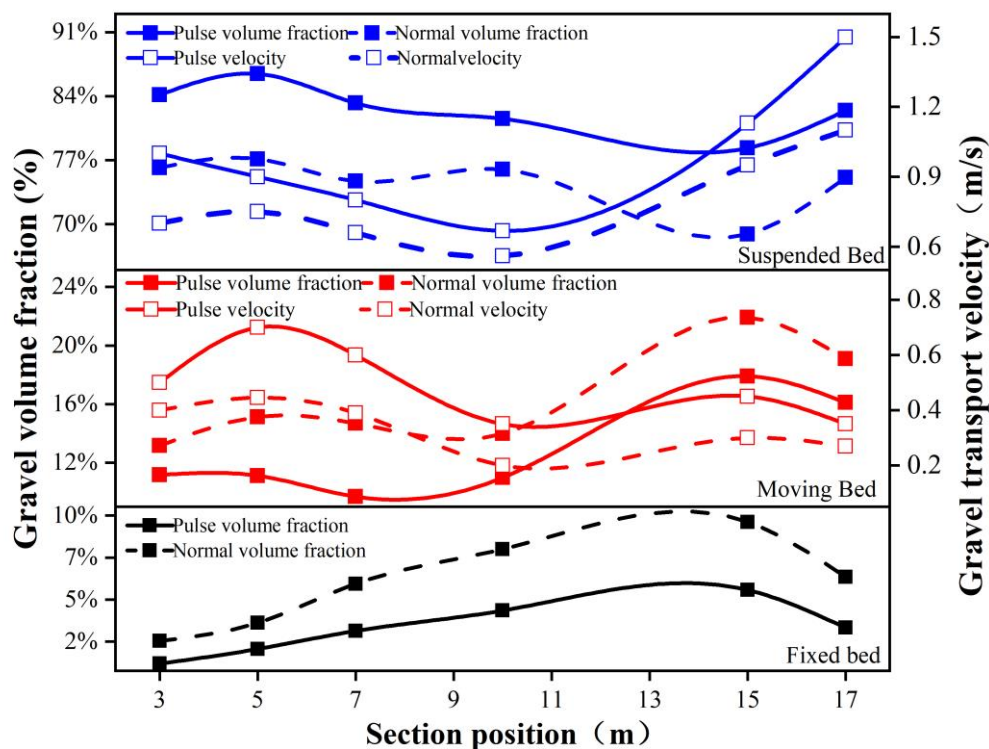


Figure 7. Graph of volume fraction and migration velocity for pulsed gravel packs and convention's in horizontal wells

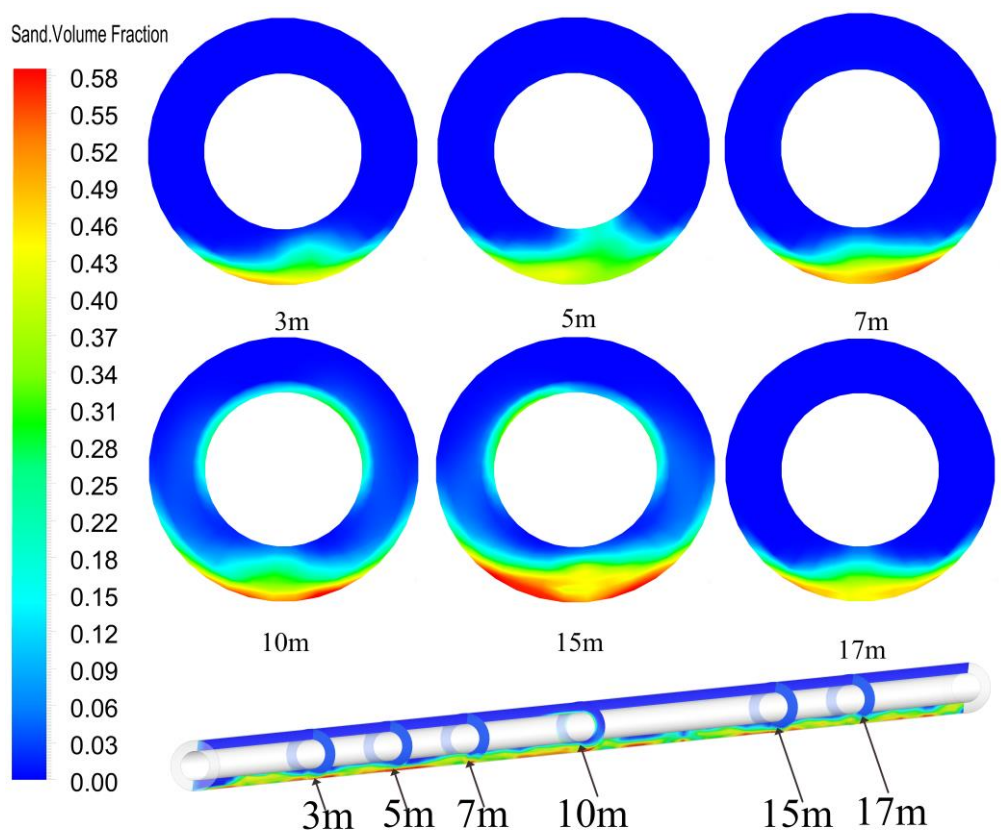


Figure 8. The contour of volume fraction for pulsed gravel packing in horizontal wells

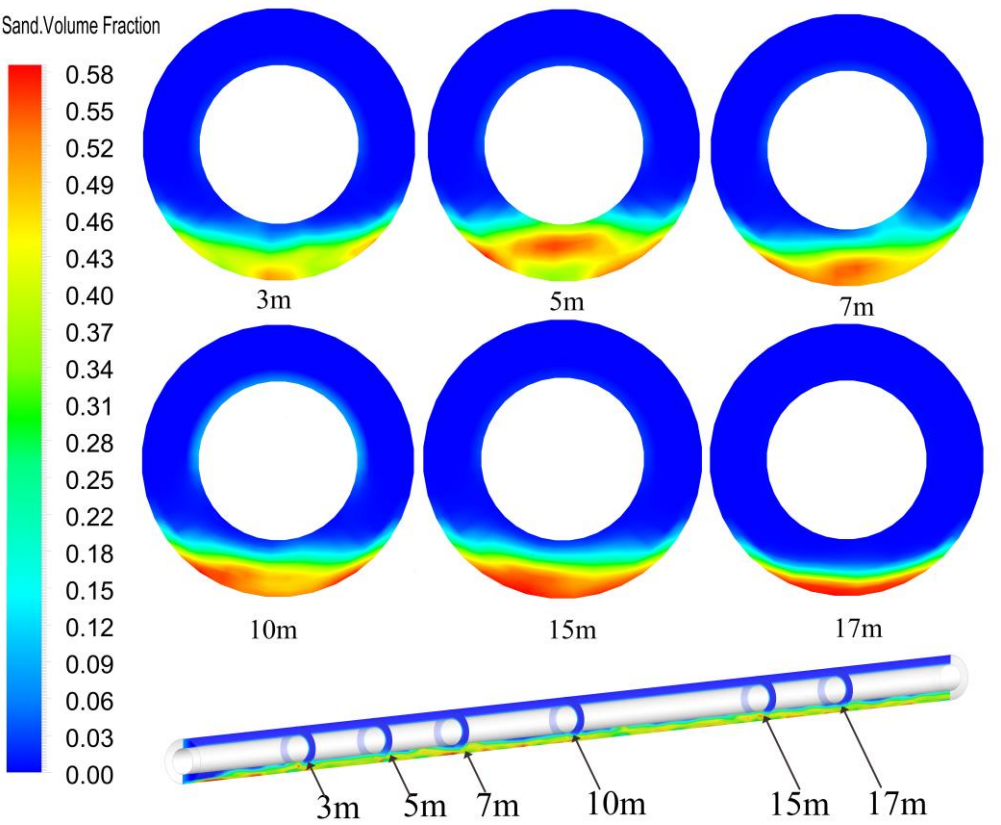


Figure 9. The contour of volume fraction for conventional gravel packing in horizontal wells

3 Analysis of influencing factors for the pulsed gravel packing

3.1 Impact of displacement on pulsed gravel packing in horizontal wells

The optimized sinusoidal pulse waveform is added to the inlet boundary to make the inlet displacement changes in pulse, and the influence of average inlet displacement from 25 m³/h to 70 m³/h on gravel migration and volume fraction was studied. At 30 s, extracting the volume fraction and velocity of the section at a distance of 10 m from the inlet, and the results were shown in Figure 10 and Figure 11. It can be seen from Figure 10, with the increase of displacement, the volume fraction of fixed bed decreased from 6.38% to 1.83%, when the displacement reaches 50 m³/h, the reduction trend of fixed bed volume fraction tends to be flat. The volume fraction of the mobile bed also decreases gradually with the increase of displacement, and when the displacement reaches 60 m³/h, the reduction trend of the volume fraction of the mobile bed increases. The volume fraction of the floating bed increases rapidly with the increase of displacement. The results indicate that with the increase of displacement, the gravel migration ability increases, and after the displacement reaches a certain critical value, the gravel migration ability increases slowly.

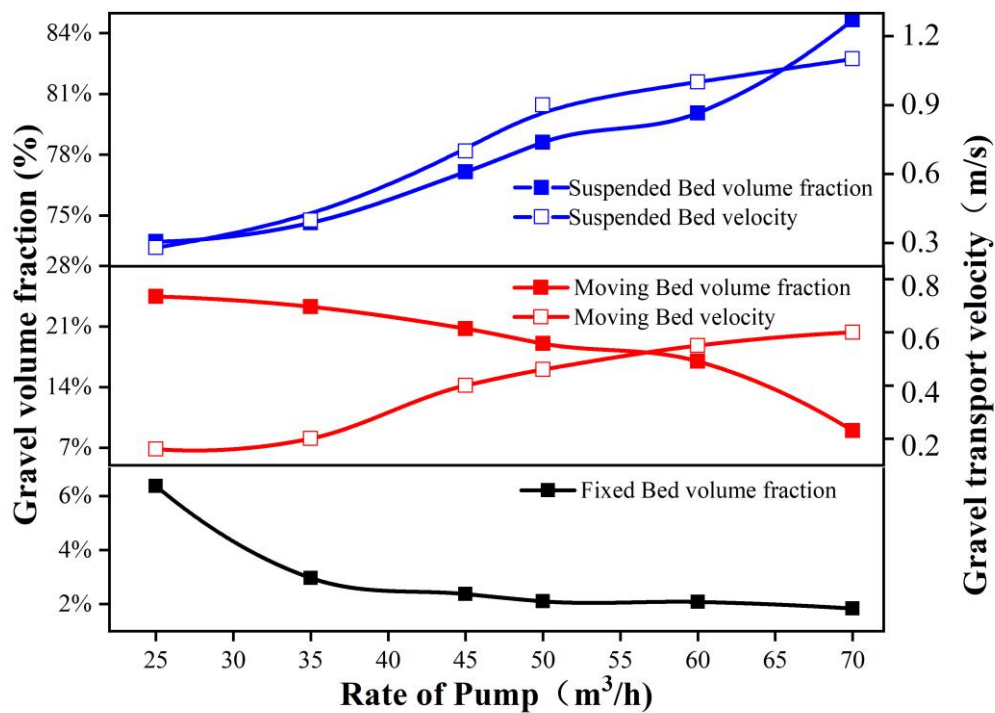


Figure 10. Graph of the effect of displacement on the volume fraction and migration velocity

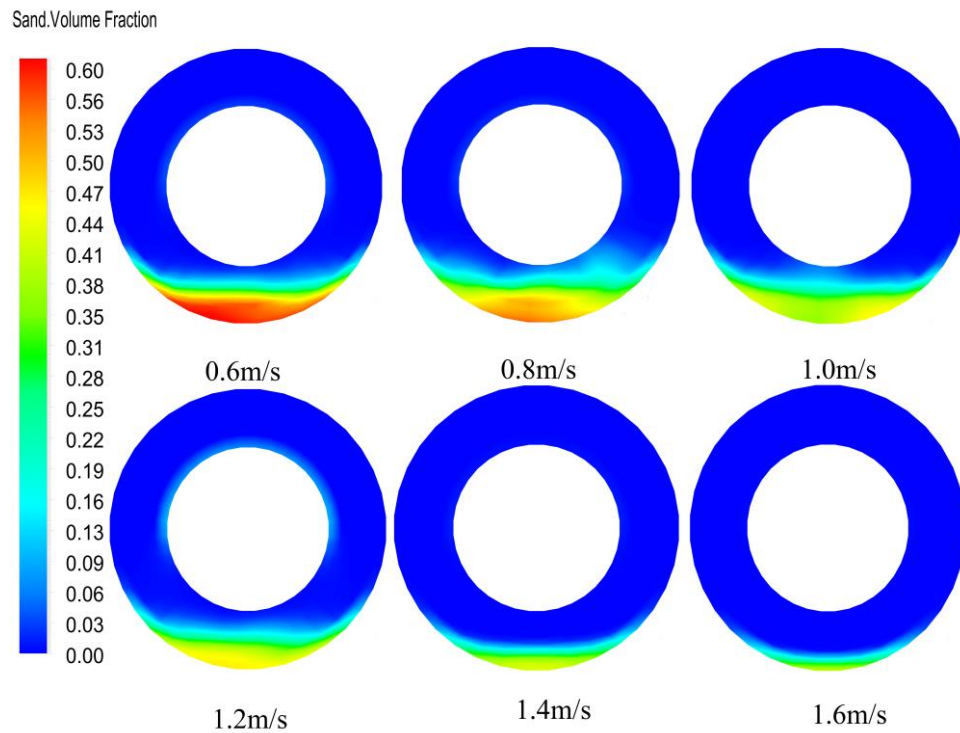


Figure 11. The contour of the effect of displacement on the volume fraction

3.2 Impact of the viscosity of the carrying fluid on pulsed gravel packing in horizontal wells

The optimized sinusoidal pulse waveform is added to the inlet boundary to make the inlet displacement changes in pulse and studying the effect of viscosity change of sand-carrying fluid on gravel migration and volume fraction. At 30 s, extracting the volume fraction and velocity of the section at a distance of 10 m from the inlet, and the results were shown in Figure 12 and Figure 13. It can be seen from Figure 12, with the increase of the viscosity of the sand-carrying fluid, the volume fraction of the fixed bed gradually decrease, and when the viscosity of the sand-carrying fluid is greater than 0.9 MPa·s, the reduction trend of the volume fraction of the fixed bed was gentle. The volume fraction of the moving bed gradually decreases with the increase of the viscosity of the sand-carrying fluid, and when the viscosity of the sand-carrying fluid is greater than 0.6 MPa·s, the decreasing trend of the volume fraction of the moving bed is gentle. The volume fraction of the suspended bed increased from 50% to 92% with the increase of the viscosity of the sand-carrying fluid, and the increase rate is the highest when the viscosity of the sand-carrying fluid was 0.6 MPa·s. The velocity of the moving bed and suspended bed also increase with the increasing of the viscosity of the sand-carrying fluid. The study shows that the viscosity of the carrier fluid increases, the energy obtained by a single gravel increases, and the transportability of gravel increases. When the viscosity of sand-carrying fluid reaches a certain critical value, the improvement of gravel transportability is relatively slow.

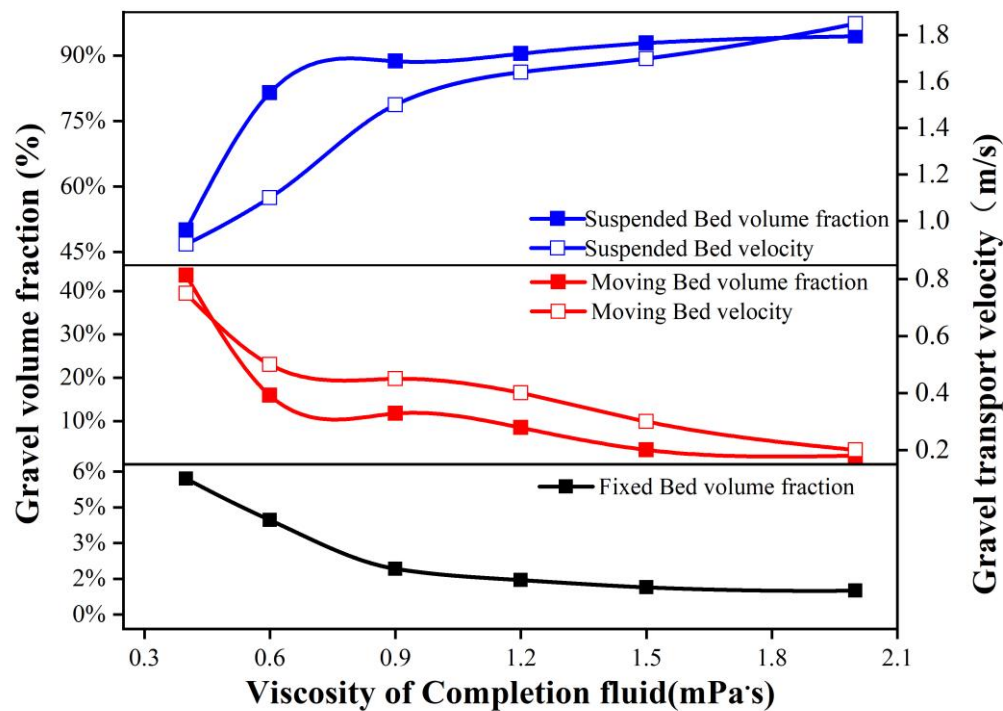


Figure 12. Graph of the effect of carrying-fluid viscosity on the volume fraction and transport velocity

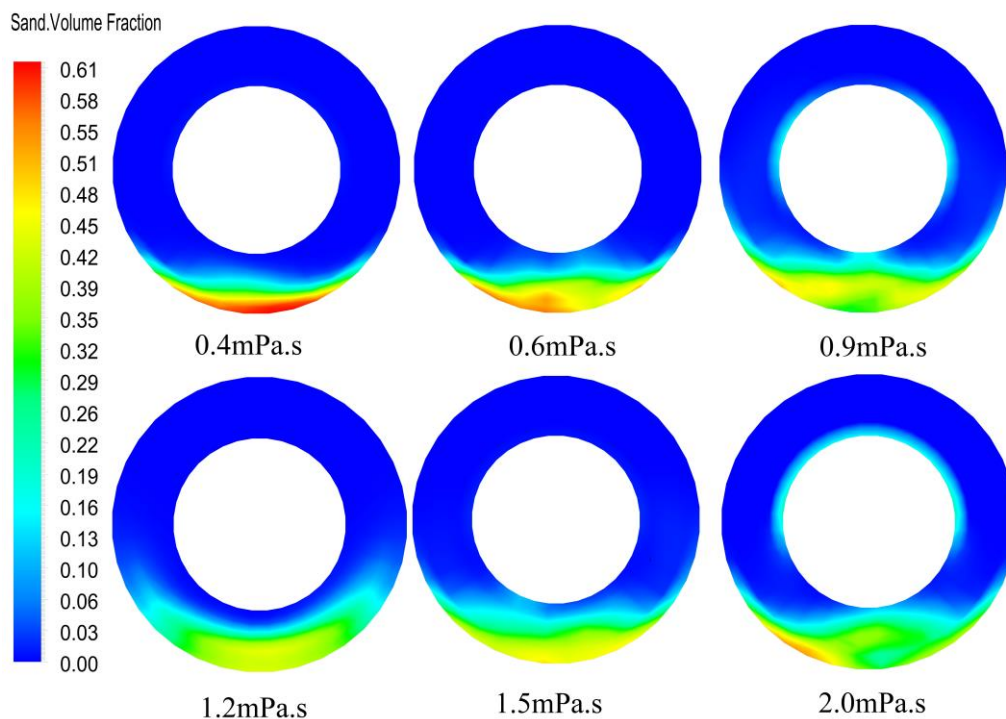


Figure 13. The contour of the effect of carrying-fluid viscosity on the volume fraction

3.3 Impact of particle size on pulsed gravel packing in horizontal wells

The optimized sinusoidal pulse waveform is added to the inlet boundary to make the inlet displacement changes in pulse and studying the effect of particle size on gravel migration and volume fraction. At 30 s, extracting the volume fraction and velocity of the section at a distance of 10 m from the inlet, and the results were shown in Figure 14 and Figure 15. It can be seen from Figure 14, with the increase of gravel diameter, the volume fraction of the fixed bed and moving bed show an increasing trend. The fixed bed volume fraction reaches the

minimum value of 2.74% when the gravel diameter is 1 mm, and the maximum value of 7.10% when the gravel diameter is 6 mm. With the increase of gravel diameter, the mobile bed volume fraction increase from 8.2% to 28%. The volume fraction of the suspended bed decreases rapidly with the increase of gravel diameter from 86% to 75%. The above results show that as the gravel diameter increases, the mass of the single gravel increases, and the energy required for the gravel transition from the static state to the mobile state increases. As the displacement of the sand-carrying fluid does not change, with the increase of gravel diameter, there is insufficient energy for the gravel to move forward. Therefore, the migration velocity of the suspended bed and the moving bed decreases obviously, which is not conducive to gravel migration.

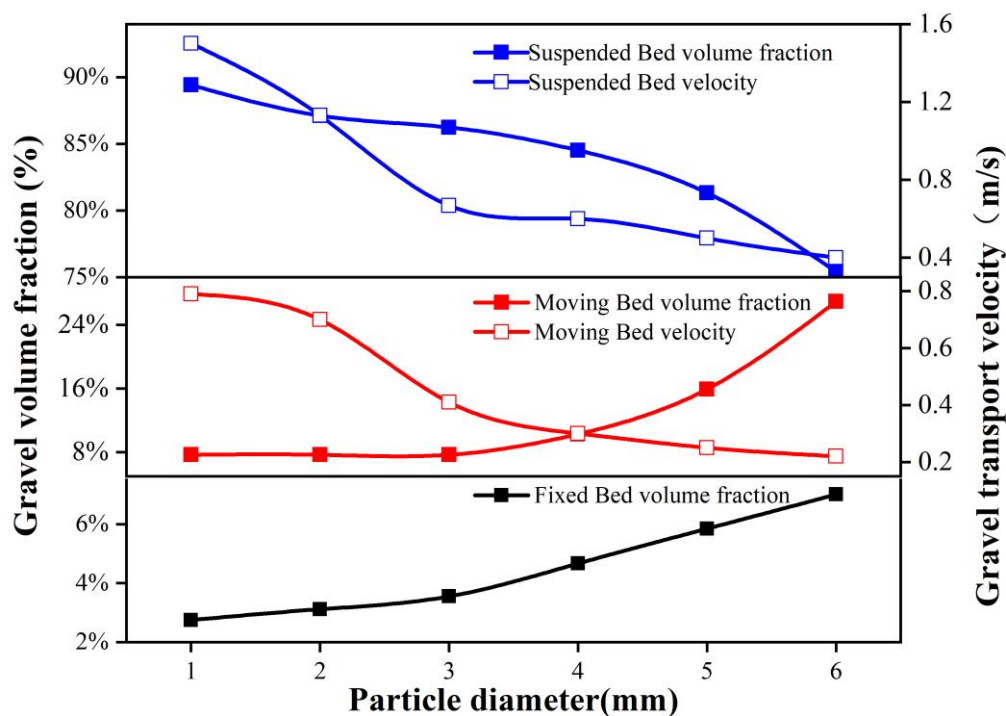


Figure 14. Graph of the effect of particle size on volume fraction and migration velocity

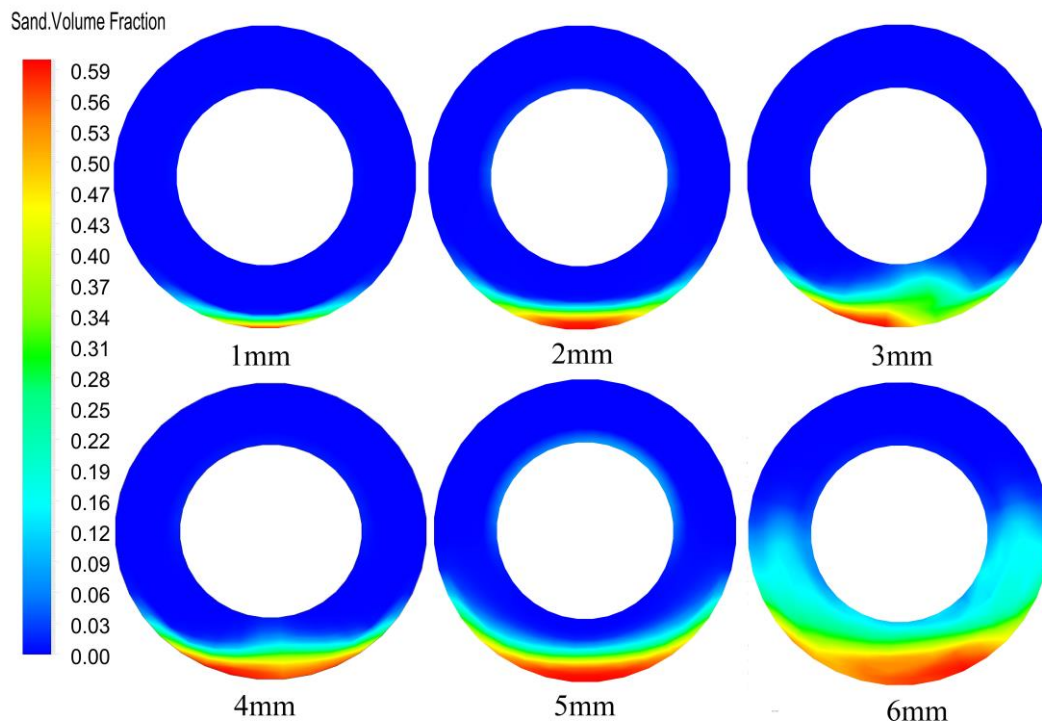


Figure 15. The contour of the effect of particle size on the volume fraction

3.4 Impact of sand carrying ratio on pulsed gravel packing in horizontal wells

The optimized sinusoidal pulse waveform is added to the inlet boundary to make the inlet displacement changes in pulse and studying the effect of sand carrying ratio on gravel migration and volume fraction. At 30 s, extracting the volume fraction and velocity of the section at a distance of 10 m from the inlet, and the results were shown in Figure 16 and Figure 17. It can be seen from Figure 16, with the increase of the sand carrying ratio, the volume fraction of the fixed bed increased from 1.6% to 6.3%, and when the sand carrying ratio reached 8%, the volume fraction increased significantly. The volume fraction of the moving bed increased from 12% to 19.5% with the increase of the carrying ratio, and the increase rate of the volume fraction increased significantly when the carrying ratio reached 7%. The volume fraction of the suspended bed decreased with the increase of the carrying ratio, and the rate of decrease increased when the carrying ratio was 7%. The transport velocity of moving bed and suspended bed decreases with the increase of sand carrying ratio. The above results show that with the increasing of the carrying ratio, the volume fraction of the moving bed and the fixed bed increase continuously, while the volume fraction of the suspended bed decreases continuously, and the transport velocity of the moving bed and the suspended bed decrease continuously. Therefore, it is necessary to strictly control the carrying ratio during pulsed gravel packing in horizontal wells.

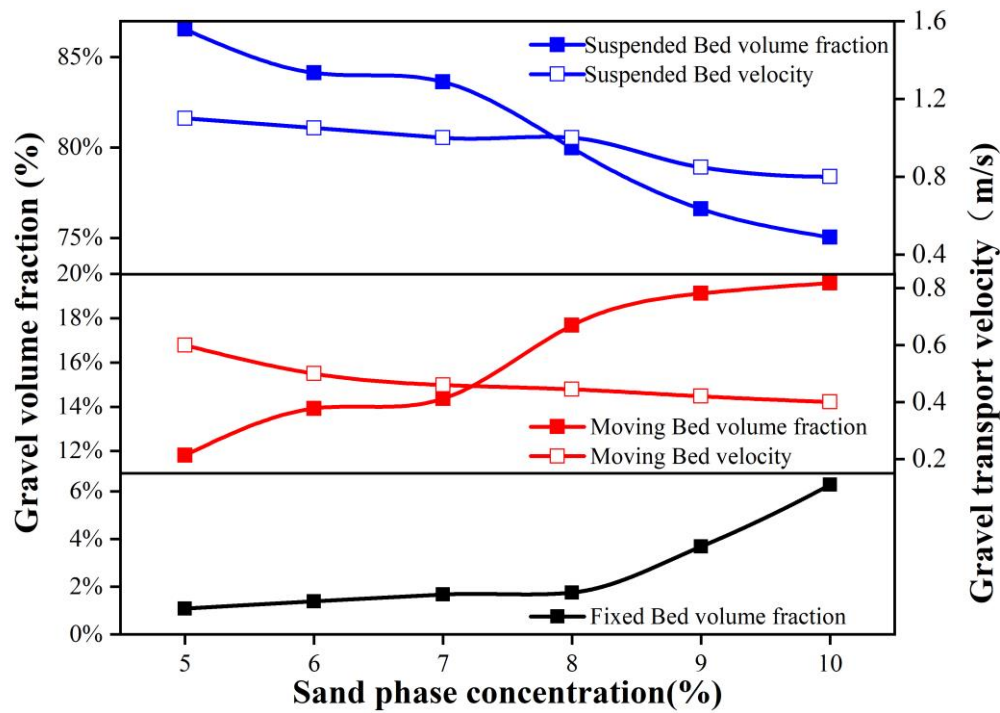


Figure 16. Graph of the effect of carrying ratio on the volume fraction and migration velocity

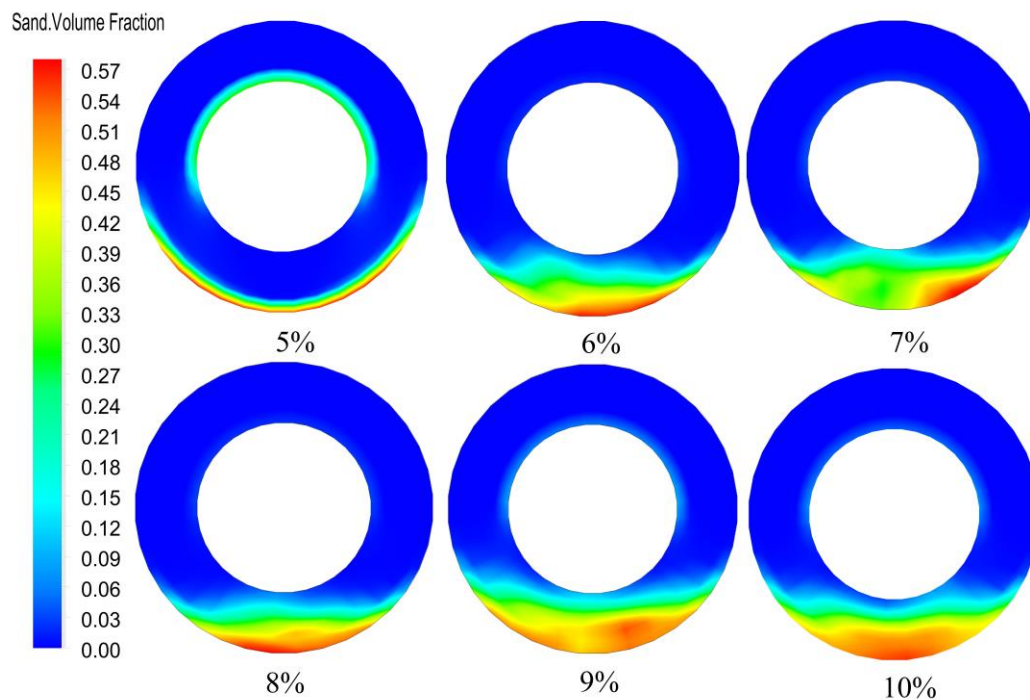


Figure 17. The contour of the effect of sand carrying ratio on the volume fraction

3.5 Impact of string eccentricity on pulsed gravel packing in horizontal wells

The optimized sinusoidal pulse waveform is added to the inlet boundary to make the inlet displacement changes in pulse and studying the effect of string eccentricity on gravel migration and volume fraction. At 30 s, extracting the volume fraction and velocity of the section at a distance of 10 m from the inlet, and the results were shown in Figure 18 and Figure 19. It can be seen from Figure 18, as the eccentricity of the string increases, the volume fraction of the fixed bed gradually increases, and when the eccentricity of the string is 0.5, the maximum

value of the volume fraction of the fixed bed is 5.70%. The volume fraction of the moving bed increases gradually with the eccentricity of the string increasing, and the maximum value is 22.5%. The volume fraction of the suspended bed decreases with the increase of the eccentricity of the string. The results show that with the increase of the eccentricity of the string, the volume fraction of fixed bed and moving bed increases, the volume fraction of suspended bed decreases continuously, and the migration velocity of moving bed decreases continuously, and the migration ability of gravel decreases.

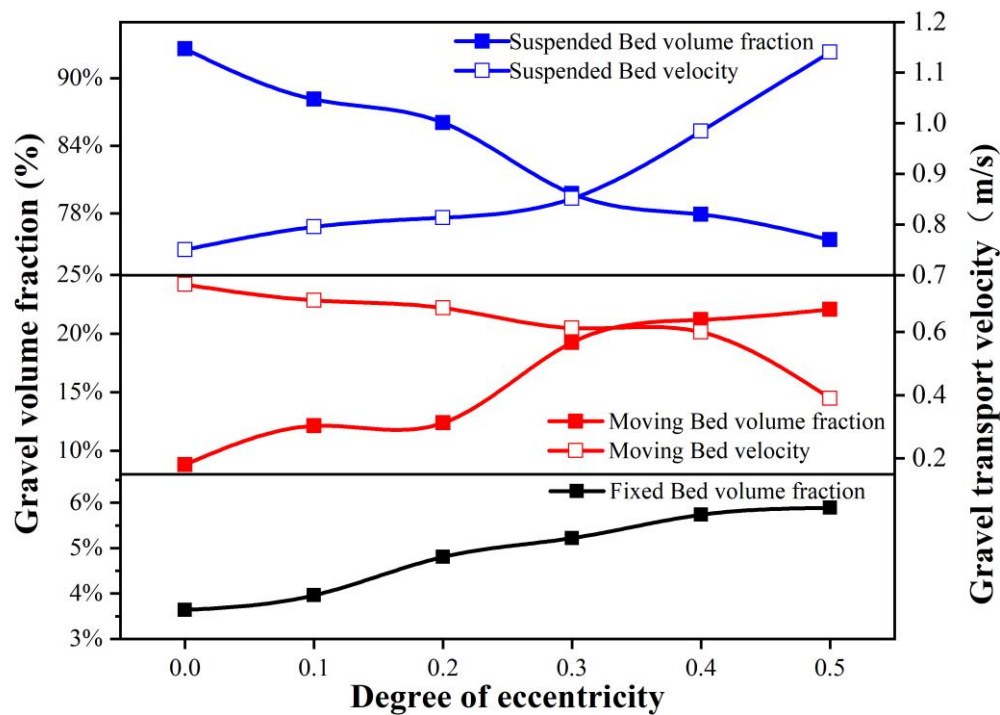


Figure 18. Graph of the effect of string eccentricity on volume fraction and migration velocity

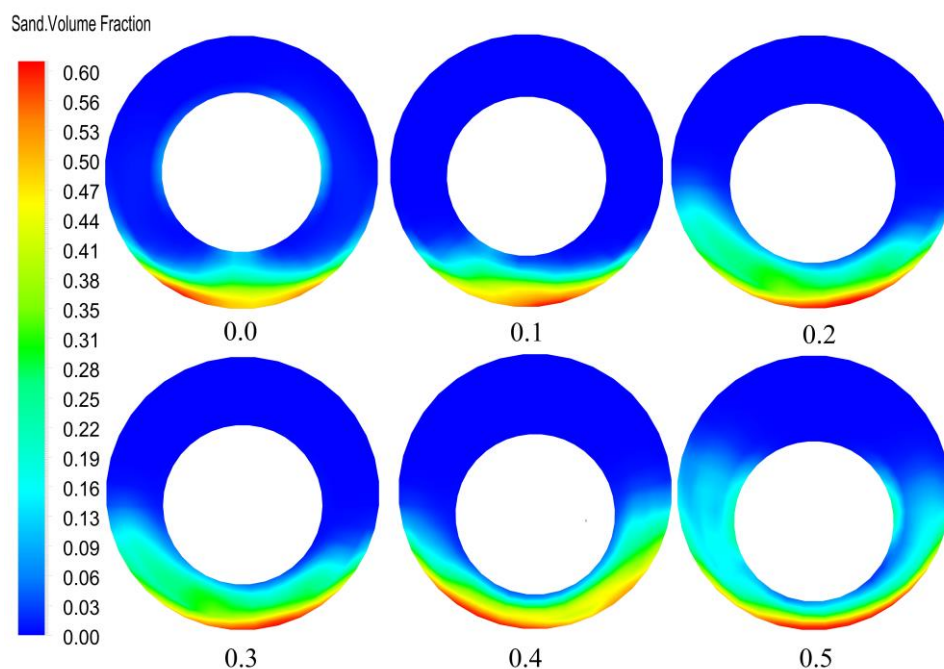


Figure 19. The contour of the effect of string eccentricity on the volume fraction

4 Conclusion

(1) By optimizing the pulsed gravel packing waveform of the horizontal well, the best sinusoidal pulse waveform is obtained, in which the frequency is 5 Hz and the amplitude is 1.65 m/s. Under this frequency and amplitude, the sand-carrying fluid has good sand-carrying performance and the best effect of reducing the volume fraction of the fixed bed, and the risk of plugging during the filling process is small and the filling efficiency is high.

(2) A comparative analysis of the results of pulsed gravel packing and conventional gravel packing in horizontal wells shows that pulsed gravel packing is more efficient than conventional gravel packing. Pulsed gravel packing has a better effect in reducing sand bed height and lengthening gravel migration distance.

(3) By analyzing the influences of the displacement of the carrying fluid, the viscosity of the carrying fluid, the gravel diameter, the carrying ratio, and the string eccentricity on the pulsed gravel packing in horizontal wells, the distribution rules of the gravel transport velocity and the volume fraction are obtained. In the process of pulsed gravel packing in horizontal wells, with the increase of displacement and viscosity of the sand-carrying fluid, the volume fraction of fixed bed and moving bed decreases gradually, while the volume fraction of suspended bed increases gradually, and the gravel transport velocity is improved. With the increase of gravel particle size, sand carrying ratio, and string eccentricity, the volume fraction of fixed bed and moving bed gradually increase, while that of suspended bed gradually decreases, and when the gravel diameter is greater than 3 mm and the sand carrying ratio is greater than 8%, the volume fraction of fixed bed rapidly increases, which may lead to the over-high sand bed. The string eccentricity has a great influence on pulsed gravel packing in horizontal wells, so it is necessary to avoid pipe eccentricity during the operation.

Author Contributions: Conceptualization, J.Y., S.C. and Q.B.; Data curation, Y.C.; Supervision, X.Q. and Y.G.; Writing—original draft, Z.Z. All authors have read and agreed to the published version of the manuscript.

Funding: This work has been supported by the Natural Science Foundation of China (NSFC: No. 51434009 and No. 51774301), the major projects of National Science and Technology (No. 2016ZX05024005) and China Scholarship Council (CSC).

Conflicts of Interest: The authors declare no conflict of interest.

Reference

1. Joshi, S.D. In Cost/Benefits of Horizontal Wells, SPE Western Regional/AAPG Pacific Section Joint Meeting, Long Beach, CA, USA, 19-24 May 2003. [<http://doi.org/10.2118/83621-MS>]
2. Alekperov, V.Y.; Lyashko, N.N.; Gavura, A.V.; Fedotov, I.B.; Kibalenko, I.A. Application of horizontal wells to accelerate commissioning of wells and to increase development efficiency of offshore oil and gas fields in the Northern Caspian (Russian). *Oil Industry Journal*. **2018**, *2018*, 72-76. [<https://www.onepetro.org/journal-paper/OIJ-2017-12-080-082-RU>]
3. Ali, S.A.; Grigsby, T.F.; Vitthal, S. Advances in Horizontal Openhole Gravel Packing. *SPE Drilling & Completion*. **2006**, *21*, 23-31. [<https://doi.org/10.2118/83995-PA>]
4. Parlar, M.; Albino, E.H. Challenges, Accomplishments, and Recent Developments in Gravel Packing. *Journal of Petroleum*

- Technology*. **2000**, 52, 50-58. [<https://doi.org/10.2118/57474-JPT>]
5. Forrest, J.K. In Horizontal Gravel Packing Studies in a Full-Scale Model Wellbore, SPE Annual Technical Conference and Exhibition, New Orleans, LA, USA, 23-26 September 1990. [<https://doi.org/10.2118/20681-MS>]
 6. Maly, G.P.; Robinson, J.P.; Laurie, A.M. New Gravel Pack Tool for Improving Pack Placement. *Journal of Petroleum Technology*. **1974**, 26, 19-24. [<https://doi.org/10.2118/4032-PA>]
 7. Doron, P.; Granica, D.; Barnea, D. Slurry flow in horizontal pipes—experimental and modeling. *International Journal of Multiphase Flow*. **1987**, 13, 535-547. [[https://doi.org/10.1016/0301-9322\(87\)90020-6](https://doi.org/10.1016/0301-9322(87)90020-6)]
 8. Doron, P.; Barnea, D. Effect of the no-slip assumption on the prediction of solid-liquid flow characteristics. *International Journal of Multiphase Flow*. **1992**, 18, 617-622. [[https://doi.org/10.1016/0301-9322\(92\)90055-L](https://doi.org/10.1016/0301-9322(92)90055-L)]
 9. Doron, P.; Barnea, D. A three-layer model for solid-liquid flow in horizontal pipes. *International Journal of Multiphase Flow*. **1993**, 19, 1029-1043. [[https://doi.org/10.1016/0301-9322\(93\)90076-7](https://doi.org/10.1016/0301-9322(93)90076-7)]
 10. Gruesbeck, C.; Salathiel, W.M.; Echols, E.E. Design of Gravel Packs in Deviated Wellbores. *Journal of Petroleum Technology*. **1979**, 31, 109-115. [<https://doi.org/10.2118/6805-PA>]
 11. Peden, J.M.; Russell, J.; Oyeneyin, M.B. In The Design and Optimisation of Gravel Packing Operations in Deviated Wells, European Petroleum Conference, London, UK, 22-25 October 1984. [<https://doi.org/10.2118/12997-MS>]
 12. Peden, J.M.; Russell, J.; Oyeneyin, M.B. In A Numerical Approach to the Design of a Gravel Pack for Effective Sand Control in Deviated Wells, SPE Annual Technical Conference and Exhibition, Houston, TX, USA, 16-19 September 1984. [<https://doi.org/10.2118/13084-MS>]
 13. Peden, J.M.; Russell, J.; Oyeneyin, M.B. In Design of an Effective Gravel Pack for Sand Control: A Numerical Approach, SPE California Regional Meeting, Bakersfield, CA, USA, 27-29 March 1985. [<https://doi.org/10.2118/13647-MS>]
 14. Wahlmeier, M.A.; Andrews, P.W. Mechanics of Gravel Placement and Packing: A Design and Evaluation Approach. *SPE Production Engineering*. **1988**, 3, 69-82. [<https://doi.org/10.2118/16181-PA>]
 15. Chen, Z. In Horizontal Well Gravel Packing: Dynamic Alpha Wave Dune Height Calculation and Its Impact on Gravel Placement Job Execution, SPE Annual Technical Conference and Exhibition, Anaheim, CA, USA, 11-14 November 2007. [<https://doi.org/10.2118/110665-MS>]
 16. Penberthy, W.L., Jr.; Bickham, K.L.; Nguyen, H.T.; Paulley, T.A. Gravel Placement in Horizontal Wells. *SPE Drilling & Completion*. **1997**, 12, 85-92. [<https://doi.org/10.2118/31147-MS>]
 17. Penberthy, W.L., Jr. Gravel Placement Through Perforations and Perforation Cleaning for Gravel Packing. *Journal of Petroleum Technology*. **1988**, 40, 229-236. [<https://doi.org/10.2118/14161-PA>]
 18. Osisanya, S.O.; Ayeni, K.B.; Osisanya, K.P. In Factors Affecting Horizontal Well Gravel-Pack Efficiency, SPE Annual Technical Conference and Exhibition, San Antonio, TX, USA, 24-27 September 2006. [<https://doi.org/10.2118/103293-MS>]
 19. Nguyen, P.D.; Fitzpatrick, H.J.; Woodbridge, G.A.; Reidenbach, V.G. In Analysis of Gravel Packing Using 3-D Numerical Simulation, SPE Formation Damage Control Symposium, Lafayette, LA, USA, 26-27 February 1992. [<https://doi.org/10.2118/23792-MS>]
 20. Martins, A.L.; Magalhaes, J.V.M.; Calderon, A.; Chagas, C.M. A Mechanistic Model for Horizontal Gravel Pack Displacement. *SPE Journal*. **2005**, 10, 229-237. [<https://doi.org/10.2118/82247-MS>]
 21. Pu, C.S. In A New Intelligent Computer System for Horizontal Wells Gravel-Packing, International Conference on Horizontal Well Technology, Calgary, Alberta, CAN, 18-20 November 1996. [<https://doi.org/10.2118/37113-MS>]
 22. Ojo, K.P.; Osisanya, S.O.; Ayeni, K.B. In Development of a 3D Numerical Simulator of Horizontal Well Gravel Pack, Canadian International Petroleum Conference, Calgary, Alberta, CAN, 13-15 June 2006. [<https://doi.org/10.2118/2006-075>]
 23. Ojo, K.P.; Osisanya, S.O.; Ayeni, K. Factors Affecting Horizontal Well Gravel Pack Efficiency. *Journal of Canadian Petroleum Technology*. **2008**, 47, 50-54. [<https://doi.org/10.2118/08-12-50>]
 24. Changyin, D.; Jiajia, L.; Yanlong, L.; Huaiwen, L.; Lifei, S. In Experimental and Visual Simulation of Gravel Packing in Horizontal and Highly Deviated Wells, SPE Latin America and Caribbean Petroleum Engineering Conference, Maracaibo, Venezuela, 21-23 May 2014. [<https://doi.org/10.2118/169237-MS>]
 25. Dong, C.Y.; Gao, K.G.; Dong, S.X.; Shang, X.S.; Wu, Y.X.; Zhong, Y.X. A new integrated method for comprehensive performance of mechanical sand control screens testing and evaluation. *Journal of Petroleum Science and Engineering*. **2017**, 158, 775-783. [<https://doi.org/10.1016/j.petrol.2017.08.043>]

26. Dong, C.Y.; Zhou, Y.G.; Chen, Q.; Zhu, C.M.; Li, Y.L.; Li, X.B.; Liu, Y.B. Effects of fluid flow rate and viscosity on gravel-pack plugging and the optimization of sand-control wells production. *Petroleum Exploration and Development*. **2019**, *46*, 1251-1259. [[https://doi.org/10.1016/S1876-3804\(19\)60278-8](https://doi.org/10.1016/S1876-3804(19)60278-8)]
27. Adamczyk, W.P.; Klimanek, A.; Białecki, R.A.; Węcel, G.; Kozołub, P.; Czakiert, T. Comparison of the standard Euler–Euler and hybrid Euler–Lagrange approaches for modeling particle transport in a pilot-scale circulating fluidized bed. *Particuology*. **2014**, *15*, 129-137. [<https://doi.org/10.1016/j.partic.2013.06.008>]
28. Pang, B.X.; Wang, S.Y.; Liu, G.D.; Jiang, X.X.; Lu, H.L.; Li, Z.J. Numerical prediction of flow behavior of cuttings carried by Herschel-Bulkley fluids in horizontal well using kinetic theory of granular flow. *Powder Technology*. **2018**, *329*, 386-398. [<https://doi.org/10.1016/j.powtec.2018.01.065>]
29. Ravnik, J.; Škerget, L.; Hriberšek, M. The wavelet transform for BEM computational fluid dynamics. *Engineering Analysis with Boundary Elements*. **2004**, *28*, 1303-1314. [<https://doi.org/10.1016/j.enganabound.2004.05.002>]
30. Wodołański, A.; Skiba, J.; Zarębska, K.; Polański, J.; Smolinski, A. CFD Modeling of the Catalyst Oil Slurry Hydrodynamics in a High Pressure and Temperature as Potential for Biomass Liquefaction. *Energies*. **2020**, *13*, 5694. [<http://dx.doi.org/10.3390/en13215694>]
31. Ofei, T.; Irawan, S.; Pao, W. CFD Method for Predicting Annular Pressure Losses and Cuttings Concentration in Eccentric Horizontal Wells. *Journal of Petroleum Engineering*. **2014**, *2014*, 1-16. [<http://dx.doi.org/10.1155/2014/486423>]
32. Argyropoulos, C.D.; Markatos, N.C. Recent advances on the numerical modelling of turbulent flows. *Applied Mathematical Modelling*. **2015**, *39*, 693-732. [<https://doi.org/10.1016/j.apm.2014.07.001>]
33. Costamte, Y.R.; Trondsen, A.; Bergkvam, R.M.; Hodne, H.; Saasen, A. In Horizontal Openhole Gravel Packing in Wells With Long Blank Pipe and Screen Sections, SPE Deepwater Drilling and Completions Conference, Galveston, TX, USA, 20-21 June 2010. [<https://doi.org/10.2118/150546-MS>]
34. Vaziri, E.; Simjoo, M.; Chahardowli, M. Application of foam as drilling fluid for cuttings transport in horizontal and inclined wells: A numerical study using computational fluid dynamics. *Journal of Petroleum Science and Engineering*. **2020**, *194*, 107325. [<https://doi.org/10.1016/j.petrol.2020.107325>]
35. Vincent, S.; Caltagirone, J.; Lubin, P.; Randrianarivelo, N. In Local Mesh Refinement and Penalty Methods Dedicated to the Direct Numerical Simulation of Incompressible Multiphase Flows, Proceedings of the ASME/JSME 2003 4th Joint Fluids Summer Engineering Conference, Honolulu, HI, USA, July 6–10 2003. [<https://doi.org/10.1115/FEDSM2003-45667>]
36. Patankar, S.V.; Spalding, D.B. A calculation procedure for heat, mass and momentum transfer in three-dimensional parabolic flows. *International Journal of Heat and Mass Transfer*. **1972**, *15*, 1787-1806. [[https://doi.org/10.1016/0017-9310\(72\)90054-3](https://doi.org/10.1016/0017-9310(72)90054-3)]